Influence of Indenter Diameter on Dynamic Indentation Tests of PEGT and PA6 Thermoplastics

Milton F. Coba Salcedo[1], Carlos Acevedo Peñaloza [2] and Gaudy Prada Botia[3]

[1] Materials Engineering and Manufacturing Technology Research Group–IMTEF
Universidad del Atlántico, Carrera 30 Número 8-49, Puerto Colombia–Colombia

[2] Mechanical Engineering Department, Faculty of Engineering
Universidad Francisco de Paula Santander

[3] Industrial Engineering Department, Engineering Faculty
Universidad Francisco de Paula Santander, Colombia

Abstract

In this article the results of the impact characterization of PETG and PA6 thermoplastics are presented, they have been characterized statically and dynamically by the indentation test, and mathematical models developed in previous works have also been used to adjust the obtained models. The Indenter diameter of the impactor used were studied. The results have shown that the specimen thickness influences the value of some of the measured properties as the thickness increases, as well as that the impactor mass influences the velocity that is printed during the test run.

Keywords: Impact resistance, Indentation test, PETG, PA6

1 Introduction

The impact of materials is undoubtedly the object of research, due to the dynamic condition inherent in the bodies that interact in our universe [1]. On the other hand,

the contribution of technological progress in instrumented test equipment by electronics is important for research, as it allows much more information on the evolution of the contact between the impactor and the sample to be recorded step by step. This information must be further processed and this phase of the research requires programming, modelling and simulation of the test dynamics to interpret or even predict the different phenomena that converge in the fraction of time in which the impact occurs [2]. In this sense, the objective has been to study the physical behaviour of different thermoplastic materials and their response when requested to impact and to develop a series of models that try to simulate the phenomenon, so as to help establish what happens at each stage of it [3]. Fracture processes in plastic materials are influenced by their properties [4]. Polymers do not have the structural regularity of other materials such as ceramics and metals, although some polymers have a certain crystalline structure, the presence of macromolecules makes their accommodation and cohesion strength different from that of other materials, thus influencing their mechanical properties [5]. That is to say, an essential characteristic of polymers is that they are formed by long chains of macromolecules that in turn become entangled with each other, so it can be observed that their structure, apparently a solid, is actually more similar to that of liquids [6-7]. This is why it is considered to be a new state of matter between solids and liquids, called the visco-elastic state. Because it is a very elastic solid or a very viscous liquid [8]. Due to the viscoelastic state of the polymers, the deformation mechanisms depend on time, this exclusive property of the polymers is of special relevance for their study and application, since in the search for relating the structure of the materials with their mechanical behaviour, reliable methods must be established to characterize the response of the materials in low, medium and high speed conditions [9-10-11]. Within these ranges, materials subjected to impact play an important role and require further research, along with the use of additional techniques and equipment to complement and improve existing impact tests. The impact techniques used to evaluate the impact behaviour of plastic materials have evolved ostensibly from sophisticated equipment and from classical techniques to the development of the theory of fracture mechanics [11-12-13]. References of work based on these advances are found in studies carried out on impact techniques, fracture mechanics, and characterization in quasi-static or high-speed conditions of stressing polymer materials (natural or modified) [14-15]. In the investigations of Sánchez-M [16], Jiménez-O [5] or Gámez-J [17].

2 Methodology

The equipment used throughout this project consists of a set of four interrelated artefacts to obtain the data needed to study the behaviour of the material, which consists of recording the force and time during the moment of impact. The equipment consists of the impact machine, the control knobs, the PC-impact machine data acquisition system and a personal computer. The tests were carried out with the DARTVIS impact machine (CEAST, Italy). See figure 1.

This equipment consists of two types of darts, one of 0.743 Kg of mass and the other of 0.503 Kg. The geometry of both darts is the same and consists of a 12.7mm diameter hemispherical head and a 60mm inner diameter and 80mm outer diameter support ring for the[X] specimens. The equipment is equipped with two detection systems, the first one with a 3200 N load cell of gauge type, located in the dart, and the second one with a piezoelectric sensor with a capacity of up to 4200 N. These load ranges limit the maximum load at which the test can be performed.
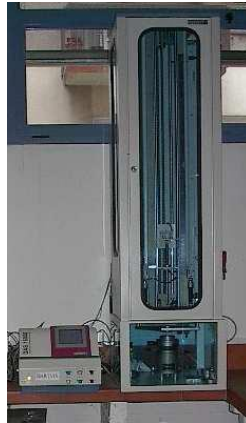

Figure 1. Impact machine test DARTVIS.

For the recorded data to be valid, the equipment must be calibrated. To do this, two actions must be carried out:
  ➢ Indicate to the data acquisition system the position where contact begins during impact.
  ➢ Have an accurate calculation of speed.
The initial velocity of impact is a basic parameter for the calculation of the coefficient of restitution. This speed can be calculated directly from the instrumentation of the equipment (V_{0i}). The equipment calculates this speed from a flag of known width (a_0) and a photoelectric cell that will record the time it takes to pass through this flag (t_b), knowing these two values, the initial speed calculated instrumentally is:

$$V_{0i} = \frac{a_O}{t_b} \tag{1}$$

This instrumentally calculated speed contains a certain experimental error, since the flag has a certain width, for small speeds precision is lost in the reading by the photoelectric cell. Another way to calculate the initial velocity is theoretically, from the drop height of the impactor dart (h) and considering it as a solid in free fall and applying the free fall equation the theoretical impact velocity V_{0t} can be calculated, where g is gravity.

$$V_{0t} = \sqrt{2 * g * h} \tag{2}$$

The values obtained by both methods are not entirely accurate and differ especially when it comes to low speeds. On the one hand, it has already been commented that by means of the first method an error is made when measuring due to the width of the flag. The other method, considering equation 2, does not take into account the friction and friction losses of the dart when falling along the guide bars, so the fall is not entirely free, making a certain error in the estimation of the actual speed. In order to be able to adjust the values of V_0 and reduce possible systematic errors, a series of measurements have been carried out by dropping the impactor in vacuum from different heights and simultaneously determining V_{oi} and V_{ot}, and by using a line of adjustment with an order of 0 at the origin, the values of V_0 are determined with greater precision by means of a correction to the free fall expression, which gives the result:

$$V_{0t} = 0.96680\sqrt{2 * g * h}
 \tag{3}$$

From now on V_0 will be the initial impact velocity, which will be corrected by equation 3. It should be noted that the setting is good enough and it is considered that more complex settings such as potentials do not provide greater precision for the velocity range used.

3. Results and discussion

A series of tests were carried out with different indenter mass, in order to check if there is any influence of the indenter geometry on the results obtained by the model. Therefore, two series of tests were carried out varying the diameter of the indenter. Two series of tests were carried out, one with a 12.7 mm diameter head and the other with a 20 mm diameter head. Figure 2 shows the elastic modulus values calculated from the serial model as a function of the initial impact velocity. In this figure it can be seen that the values are very similar, not varying significantly from one diameter to another.
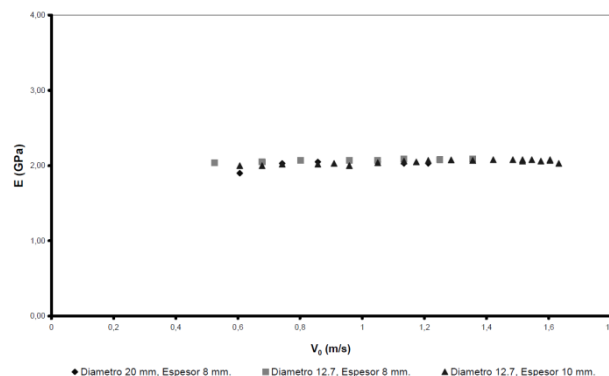

Figure 2. Influence of specimen diameter on the elastic modulus.

After studying values such as ε, Ci, E, and F_{max} in different conditions of dynamic indentation in the PETG. Measurements of the residual deformation printed on the

surface of the specimen have been made using the confocal microscopy technique, applied to indentation tests under the conditions described in Table 1. In order to compare the deformations obtained by microscopy with the deformations calculated through the serial model. In other words, it seeks to compare the experimentally obtained fingerprint with the fingerprint predicted by the model.

Table 1. Conditions of the fingerprint tests measured by confocal microscopy at PETG.

Test mm	Indenter mass (Kg)	Indenter diameter (mm)	Thickness test piece (mm)	Speed of impact V_0 (m/s)
125	0.743	12.7	10	[1.515]
130	0.743	12.7	10	[1.515]
140	0.743	12.7	10	[1.515]
145	0.743	12.7	10	[1.515]

The first test was conducted to study the shape of the print. Depending on the material and speed of the indentation, the print has different shapes. These can be classified into two groups: a) shear yielding and b) pilling up. As an example, a foam plate that is impacted by a dart, in the impact zone the material will contract without having to overflow the displaced volume at the edges, i.e. the material does not need to flow out because its structure can be compressed giving space to the indenter. This behavior is typical for polymers. However, when certain levels of stress are reached, the structure of the material will form shear bands due to its inability to continue deforming, this phenomenon is called shear yielding. Otherwise, if the material tends to flow laterally to the impact zone, forming a truncated conical surface around the footprint with the excess material, this behaviour is called pilling-up.

In figure 3, the profile of an indentation mark is observed, this mark behaves as described above by shear yielding, i.e. it does not have an accumulation or burr around the impacted area. This profile does not show anything that could give more information on the affected area. However, when looking at the indentation mark through the microscope, the formation of shear bands in the most mechanically stressed areas can be distinguished. (See Figures 3 and 4). When detailing figures 3-4 and superimposing them, it can be seen that the marks on the edges of figure 4 do not represent any physical variation of the profile, but a change in the internal structure of the polymer. That is to say, in some areas of the material when it reaches the yield limit, the chains are reoriented to favour the sliding between them, causing a change in the structure and colour.
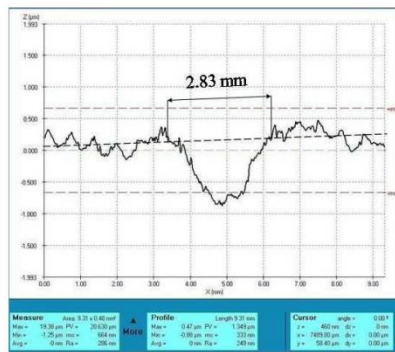
Figure 3.
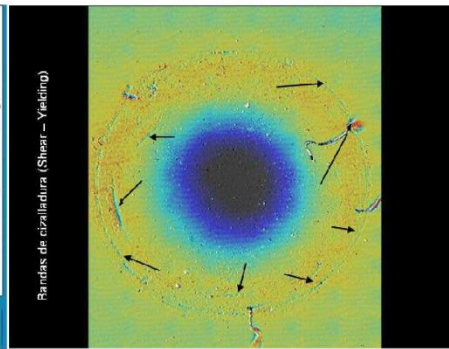Extended profile of an indentation track at a speed of 1,545 m / s.

Figure 4. Shear bands in an indentation trace obtained by confocal microscopy
.

The shear bands indicated do not have a continuous alignment across the diameter of the footprint in the form of a circle, therefore, irregular arcs are observed around its perimeter, this is due to the defects of the material itself, which cause the distribution of stresses is not symmetrical and does not form a circle. It should be noted that the diameter equivalent to the maximum penetration does not necessarily coincide with the diameter indicated by the shear bands. The diameter marked by the shear bands is imposed by the maximum shear stress the material can withstand and is independent of the maximum penetration. Once the material reaches this tension it forms the bands, but the indenter can continue to lower and penetrate further. Continuing with the previous example, in the case of pilling up tracks at the moment of impact, the impacted zone overflows material laterally as the indenter advances, making the material flow and forming the geometry shown in figure 5, in this type of track dominates the viscous behavior of the material and there is also a strong increase in friction between the material and the indenter. In the case of PETG, it will behave by pilling up, although it is negligible due to the low height of the overflowing material.
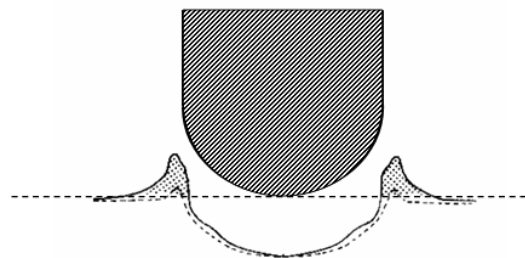

Figure 5. Pilling up characteristic footprint.

Figure 6 shows the measurements made by fingerprint microscopy on the PETG, detailing the two-dimensional topography of the impact surface and the profile corresponding to the diameter of the indentation. Also in figure 6, you can see how pilling up is negligible in PETG. If the pilling up were more marked, i.e. if

the volume of material moved was greater, the conditions of Herzt's law would not be met. Therefore, the serial model used for the calculations would not be valid for the materials evaluated.
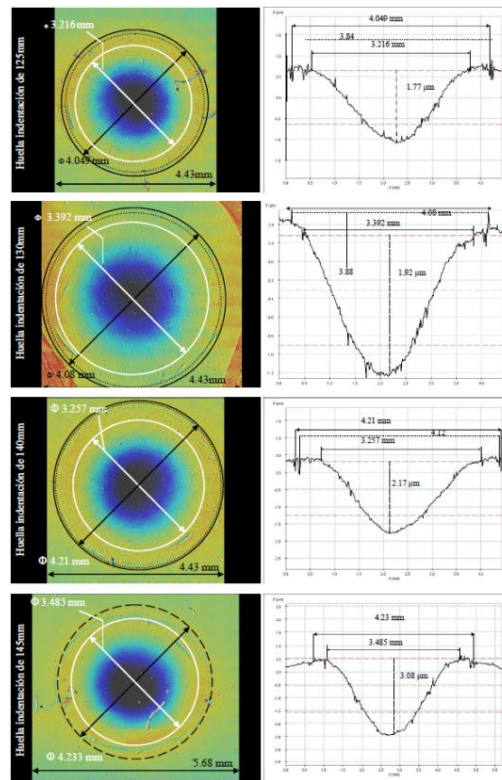

Figure 6. Extended topographies and profiles made by confocal microscopy on PETG samples tested at different indentation fall heights.

In order to establish a comparative table between the values obtained by the different techniques, table 2 was prepared, in which the values of the diameters calculated by maximum deformation (experimental and numerical), residual deformation (experimental and numerical), and confocal microscopy are listed. The experimental and theoretical diameters have been calculated from the penetration calculated by the serial model, and from the penetration given by the indenter displacement theory. Considering the known penetration (α) and the radius of the indenter (6.35 mm) by the Pythagorean theorem (Navas page 174), the diameter associated with any penetration is calculated according to equation 4.

$$6.35^2 = (6.35 - \alpha)^2 + (\emptyset/2)^2 \qquad (4)$$

Table 2. Results of experimental and theoretical measurements of fingerprints by indentation.

Test mm	$\emptyset max$ displacement (mm)	$\emptyset max$ serie (mm)	$\emptyset$ residual (mm)	$\emptyset$ residual serie (mm)	$\emptyset$ residual profile (mm)	$\emptyset$ shear yield (mm)
125	5.7142	5.6845	2.7927	3.2626	3.216	4.049
130	5.7886	5.7050	3.0684	3.3430	3.392	4.080
140	5.8604	5.8160	2.6432	3.3885	3.257	4.210
145	5.9611	5.8716	3.1402	3.5342	3.485	4.230

Table 2 shows the values of the results obtained in the tests carried out at different impact heights and from which it is established the diameter of the footprint due to the maximum displacement of the head (Ømax offset), calculated by the penetration recorded in the test, and the maximum diameter of the footprint obtained by the serial indentation model (Ømax offset) are the same. The residual diameter (Øresidual mm), measured moments after the test, the residual diameter obtained by the series indentation model (Øresidual series), and the residual diameter obtained by microscopy (Øresidual Profile), are coincident, confirming the validity of the series model. However, it can be observed that the calculated residual diameters are larger than those measured directly on the sample, this is due to the viscoelastic recovery that the material undergoes during the period of time that passes by the transfer from the test equipment to the measurement site.

The table of results also includes the column of diameters where shear yielding appears. By studying the distribution of stresses and strains between contacts between a flat plate and a sphere, this column can be useful if you want to know when the material will start to fail plastically. The [] series model has been used in the development of this investigation in indentation. Subsequently, the model was applied exhaustively to the different tests and the geometric variables involved in the test were evaluated, which allowed for a broad characterisation of the indentation behaviour of PETG. And finally, a series of tests and the respective calculations will be carried out through the simple and reinforced polyamide series model. For illustrative purposes, figure 7 shows the adjustment made to a curve obtained experimentally from polyamide 6, in which, in addition to the adjustment made by the force-time-time curve model, the deformation-time adjustments and the velocity-time curve recorded in the test are shown. This figure is representative of the adjustment made to the totality of the tests made to the simple and reinforced polyamide 6.
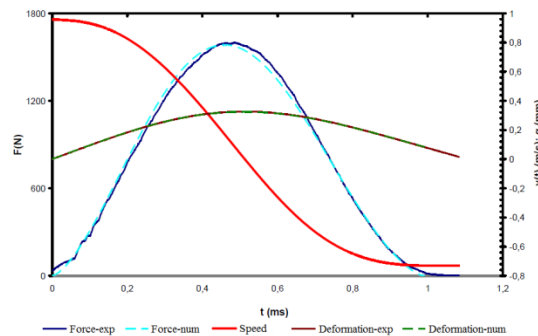
Figure 7. Adjustment of force-time, deformation-time and velocity curves of a dynamic indentation test on PA6 at a fall height of 50mm.

Once the tests have been carried out, figure 8 is presented, comparing the modules obtained in tests carried out on simple PA6 and with 22.5% and 45% fibreglass, as well as the maximum force values recorded (see figure 9), these tests were carried out with the 12.7 mm diameter head, 9 mm sample thickness and 0.503 kg indenter mass, which obey suitable parameters according to the characteristics obtained from the previous tests with PETG. The values obtained in dynamic indentation of each material, allows to advance in the mechanical characterization at high speed of solicitation.
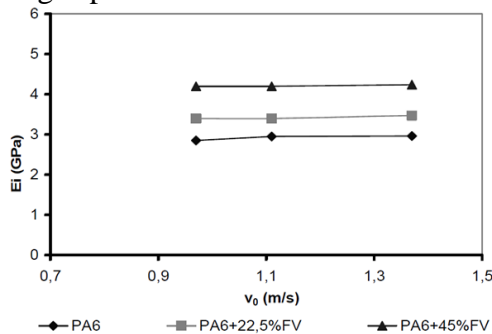

Figure 8. Elastic modules in single and reinforced PA6 dynamic indentation
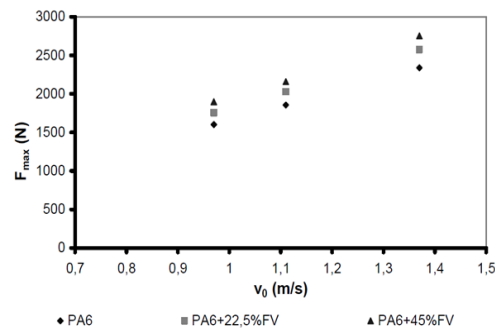

Figure 9. Maximum force recorded as a function of impact speed.

4. Conclusions

The results show a slight increase in the elastic modulus with the impact velocity, which is in accordance with the viscoelastic nature of the materials tested and with the principle of superposition in polymers, as in previous results, in indentation the fibre content is detected. Therefore, the maximum force and modulus of elasticity values increase with the percentage of fibre content. There are two important factors that this type of test provides:
➤ The test geometry normally applied to polymers requires the material to be tensile, bending, or a combination of these, however, the tests that apply or combine the stress to compression are less. For this reason, indentation provides added value to the characterization, as it provides information on the

materials to be compressed, and in the case of composite materials, it makes it possible to assess the impact of reinforcement on this type of geometry. In short, this type of test, due to the way in which it is applied, provides information on the compression behaviour and, at the same time, allows the material to be characterised in the wide range of stresses to which the material will be subjected in the applications to which it is destined.

➢ On the other hand, from the module values observed, and the type of indentation stress, we can observe an excellent coherence of the results obtained for each material depending on the amount of fibre and the tendency to comply with the law of mixtures in the different types of tests carried out so far.

References

[1]   L. Aretxabaleta, J. Aurrekoetxea, I. Urrutibeascoa, M. Sánchez-Soto, Characterisation of the impact behaviour of polymer thermoplastics, *Polymer Testing*, **24** (2005), no. 2, 145-151. https://doi.org/10.1016/j.polymertesting.2004.09.014

[2]   S. Boria, A. Scattina, G. Belingardi, Impact behavior of a fully thermoplastic composite, *Composite Structures*, **167** (2017), 63-75. https://doi.org/10.1016/j.compstruct.2017.01.083

[3]   X.C. Sun, L.F. Kawashita, A.S. Kaddour, M.J. Hiley, S.R. Hallett, Comparison of low velocity impact modelling techniques for thermoplastic and thermoset polymer composites, *Composite Structures*, **203** (2018), 659-671. https://doi.org/10.1016/j.compstruct.2018.07.054

[4]   Matthew Bondy, Pascal Pinter, William Altenhof, Experimental characterization and modelling of the elastic properties of direct compounded compression molded carbon fibre/polyamide 6 long fibre thermoplastic, *Materials & Design*, **122** (2017), 184-196. https://doi.org/10.1016/j.matdes.2017.03.010

[5]   O. A. Jiménez Arévalo, *Comportamiento A La Fractura De Composites Con Matriz De Poliestireno*, PhD Tesis, Universidad Politécnica de Cataluña. Terrassa, 2002.

[6]   Marcus Schoßig, Christian Bierögel, Wolfgang Grellmann, Thomas Mecklenburg, Mechanical behavior of glass-fiber reinforced thermoplastic materials under high strain rates, *Polymer Testing*, **27** (2008), no. 7, 893-900. https://doi.org/10.1016/j.polymertesting.2008.07.006

[7]   J.L. Thomason, The influence of fibre length, diameter and concentration on the impact performance of long glass-fibre reinforced polyamide 6,6, *Com-*

posites Part A: Applied Science and Manufacturing, **40** (2009), no. 2, 114-124. https://doi.org/10.1016/j.compositesa.2008.10.013

[8]   S. Turner, *Mechanical Testing of Plastics*, 2nd Edition, The Plastics and Rubber Institute, Londres, 1983.

[9]   Gin Boay Chai, Periyasamy Manikandan, Low velocity impact response of fibre-metal laminates – A review, *Composite Structures*, **107** (2014), 363-381. https://doi.org/10.1016/j.compstruct.2013.08.003

[10] Rafael Santiago, Wesley Cantwell, Marcílio Alves, Impact on thermoplastic fibre-metal laminates: Experimental observations, *Composite Structures*, **159** (2017), 800-817. https://doi.org/10.1016/j.compstruct.2016.10.011

[11] Norman Jones, Note on the impact behaviour of fibre-metal laminates, *International Journal of Impact Engineering*, **108** (2017), 147-152. https://doi.org/10.1016/j.ijimpeng.2017.04.004

[12] Matthew Bondy, William Altenhof, Low velocity impact testing of direct/inline compounded carbon fibre/polyamide-6 long fibre thermoplastic, *International Journal of Impact Engineering*, **111** (2018), 66-76. https://doi.org/10.1016/j.ijimpeng.2017.08.012

[13] ISO 527-2:2012(en) Plastics — Determination of tensile properties — Part 2: Test conditions for moulding and extrusion plastics.

[14] Javier Antonio Navas López. Estudio, *Evaluación Y Modelado Del Comportamiento De Indentación Y Flexión-Indentación A Impacto De Baja Energía De Materiales Termoplásticos*, PhD Thesis, Universidad Politecnica de Cataluña. Barcelona, 2008.

[15] C. Hardy, C. N. Baronet and G. V. Tordion, The elasto-plastic indentation of a half-space by a rigid sphere, *Journal of Numerical Methods in Engineering*, **3** (1971), 451-462. https://doi.org/10.1002/nme.1620030402

[16] M. Sánchez-Soto, *Comportamiento Mecánico y Fractura De Mezclas De Poliestireno y Microesferas De Vidrio*, PhD Tesis, Universitat Politècnica de Catalunya, 2000.

[17] J. Gámez Pérez, *Relación Estructura-Propiedad En Placas Y Láminas De Polipropileno Y Copolímeros En Bloque Etileno-Propileno Obtenidas Por Diferentes Procesos De Transformación*, PhD Tesis, Universitat Politècnica de Catalunya, 2006.